

PACS numbers: 42.60.Da; 42.60.Fc; 42.60.Mi; 42.55.Lt
DOI: 10.1070/QE2006v036n09ABEH013327

Self-oscillation perturbations in a fast-flow unstable resonator laser

A.I. Odintsov, N.E. Sarkarov, A.I. Fedoseev

***Abstract*. It is shown with the help of numerical simulation that various mechanisms of self-oscillation instability exist and self-oscillation perturbations of various types may appear in an unstable resonator with a transverse flow of the active medium and a nonuniform internal pumping. The interaction of different self-oscillation perturbations, manifested in pulling and locking of oscillation frequencies and a variation of their increments, is studied. Analytic relations describing the spatial structure of perturbation modes and used for evaluating their frequencies and increments from steady-state generation parameters are presented.**

Keywords: *fast-flow laser, unstable resonator, self-oscillation instability*.

1. Introduction

Self-oscillation instability of steady-state generation in an unstable resonator with a transverse flow of the active medium is due to the feedback between the axial and peripheral resonator regions produced by the moving medium [1]. In fast-flow lasers, instability is developed due to field nonuniformity in the unstable resonator, while stabilisation of steady-state generation is facilitated by uniform pumping in the resonator, energy exchange processes in the active medium, and a spread of flow velocities [2 – 5]. However, steady-state generation becomes unstable for a nonuniform pumping rate profile decreasing towards the unstable resonator axis, and the laser passes to self-modulated generation regime [6]. The pumping profile can be varied by switching the lasing modes.

Experimental data available in the literature point towards the instability of steady state generation in fast-flow lasers with an unstable resonator [7, 8]. Most of the studies were devoted to 'transit' self-oscillations whose frequencies are determined by the transit time τ_f of the medium through the resonator. It will be shown below that oscillations with a higher frequency corresponding to the transit time of the medium through a certain region in the unstable resonator can also be excited. We shall call these self-oscillations intrinsic transit oscillations. In the quasi-steady-state generation approximation, which was used for calculations in most cases, a whole range of self-oscillation perturbations associated with the growth of relaxation oscillations in an unstable resonator are neglected. Such perturbations were detected in [9] in which a more general transit model of the unstable resonator was used. For typical parameters of fast-flow CO_2 lasers, the relaxation oscillation frequency is much higher than the transit oscillation frequency.

In this paper, we analyse the instability mechanisms and the conditions for excitation of various types of self-oscillations, calculate the mode parameters of perturbation (frequencies, increments, spatial structure), and study the mutual influence of various types of self-oscillations.

A.I. Odintsov, N.E. Sarkarov, A.I. Fedoseev Department of Physics, M.V. Lomonosov Moscow State University, Vorob'evy gory, 119992 Moscow, Russia; e-mail: spekl@phys.msu.ru, nsark@triniti.ru

Received 28 November 2005; revision received 8 June 2006
Kvantovaya Elektronika **36** (9) 853 – 859 (2006)
Translated by Ram Wadhwa

2. Calculating model and basic equations

In our calculations, we used the one-dimensional geometrical optics model of an unstable resonator with cylindrical mirrors which was completely filled with an active medium. It was assumed that there are no dissipative losses in the resonator, while the losses due to magnification in $\theta = \ln M/2L$ are distributed uniformly over the length L of the resonator (M is the magnification factor per round-trip transit). The medium was described by the simplest kinetic equation with one relaxation constant.

The initial system of equations for the gain $G(x,t)$ and the field intensity $W(x,t)$ in the resonator for normalised quantities had the form

$$\frac{\partial G}{\partial t} - \frac{\partial G}{\partial x} = -\left(W + \tau_r^{-1}\right)G + q, \tag{1}$$

$$\tau_c \frac{\partial W}{\partial t} + x\frac{\partial W}{\partial x} = (G-1)W. \tag{2}$$

Here $G = \alpha/\theta$; α is the gain of the medium; $W = \sigma I \tau_f$; I is the field strength; σ is the optical transition cross section; $\tau_f = h/v$ is the transit time of the medium up to the optical axis of the resonator (h is the resonator aperture and v is the flow velocity); τ_r is the relaxation time of the medium inversion normalised to τ_f; $q = \sigma S \tau_f/\theta$ is the normalised pumping; S is the pump rate; and $\tau_c = 2L/(c\tau_f \ln M)$ is the normalised time of field attenuation in the unstable resonator. The variables t and x are normalised to τ_f and h, respectively. The steady state solutions of the system of equations (1), (2) describe the distribution of the gain $G_s(x)$ and the field intensity $W_s(x)$ in the cw lasing regime.

In accordance with the standard procedure of stability investigations, linearised equations were obtained from (1) and (2) for small relative perturbations of the steady-state solutions $\tilde{g} = \delta g(x,t)/G_s(x)$ and $\tilde{w} = \delta w(x,t)/W_s(x)$. By substituting $\tilde{g}(x,t) = \bar{g}(x)\exp(\bar{\Gamma}t)$ and $\tilde{w}(x,t) = \bar{w}(x) \times \exp(\bar{\Gamma}t)$ into these equations, we obtained equations for the complex amplitudes $\bar{g}(x)$ и $\bar{w}(x)$ of perturbation modes with the complex increment $\bar{\Gamma}$ (hereafter, the bar indicates complex quantities):

$$\frac{d\bar{g}}{dx} = \left(\bar{\Gamma} + \frac{q}{G_s}\right)\bar{g} + W_s\bar{w}, \tag{3}$$

$$x\frac{d\bar{w}}{dx} = G_s\bar{g} - \bar{\Gamma}\tau_c\bar{w}. \tag{4}$$

These equations should be solved with the following boundary conditions at the inlet to the resonator ($x = 1$): $\bar{g}(l) = 0$. It follows from (4) [taking into account $G_s(0) = 1$] that the condition

$$\frac{\bar{g}(0)}{\bar{w}(0)} = \bar{\Gamma}\tau_c \tag{5}$$

must be satisfied on the optical axis of the unstable resonator ($x = 0$).

The system of equations (3), (4) with the above boundary conditions is the boundary value problem for finding the eigenfunctions (perturbation modes) $\bar{g}(x)$ and $\bar{w}(x)$ and eigenvalues $\bar{\Gamma}$. In numerical calculations, we solved the equations for the moduli $g = |\bar{g}|$ and $w = |\bar{w}|$ and phases Φ_g and Φ_w of perturbation modes, which have the form

$$\frac{dg}{dx} = \left(\Gamma + \frac{q}{G_s}\right)g + W_s w\cos\Phi, \tag{6}$$

$$\frac{d\Phi_g}{dx} = \Omega - W_s\frac{w}{g}\sin\Phi, \tag{7}$$

$$x\frac{dw}{dx} = -\Gamma\tau_c w + G_s g\cos\Phi, \tag{8}$$

$$x\frac{d\Phi_w}{dx} = -\Omega\tau_c + G_s\frac{g}{w}\sin\Phi, \tag{9}$$

where $\Phi = \Phi_g - \Phi_w$; $\Gamma = \mathrm{Re}\,\bar{\Gamma}$; $\Omega = \mathrm{Im}\,\bar{\Gamma}$. The boundary conditions for this system at the inlet to the resonator were taken in the form

$$g(1) = 0, \quad \Phi(1) = \pi. \tag{10}$$

On the resonator axis ($x = 0$) the following relations must be satisfied:

$$\frac{g(0)}{w(0)} = |\bar{\Gamma}|\tau_c, \quad \Phi(0) = \arctan\frac{\Omega}{\Gamma}. \tag{11}$$

The system of equations (6)–(9) can be reduced to a system of two equations for the ratio $R = g/w$ and the phase difference Φ. In the special case $\tau_c = 0$, these equations are transformed into equations for the quasi-stationary model. In this case, the boundary conditions for Eqns (3) and (4) take the form $\bar{g}(0) = \bar{g}(1)$, while for Eqns (6)–(9), we obtain

$$g(0) = 0, \quad \Phi(0) = 0, \quad g(1) = 0, \quad \Phi(1) = \pi. \tag{12}$$

The pump profile descending to the unstable resonator axis was described by the relation

$$q(x) = q_m\left[1 - p\exp\left(-\frac{x^n}{h_0^n}\right)\right], \tag{13}$$

where h_0 is the width of the nonuniformity pump region ($h_0 \ll h$); q_m is the pump parameter; $p = 1 - q(0)/q_m$ is the relative depth of the pump profile dip on the unstable resonator axis; the exponent n characterises the profile steepness ($n = 2, 4$ for most calculations). The relation between the pump parameters q_m and the relaxation time τ_r, as a rule, correspond approximately to a fourfold excess over the lasing threshold ($q_m\tau_r \approx 4$) in a homogeneous medium ($p = 0$). The gain $G_s(1)$ of the medium at the inlet to the resonator was chosen equal to $q(1)\tau_r$, which corresponds to identical pump rates inside and outside the resonator.

3. Analytic model for a weakly inhomogeneous medium

If the spatial parameters of the system described by the steady-state distributions $G_s(x)$, $W_s(x)$, and $q(x)$ vary slowly on the scale of the spatial self-oscillation period $\Lambda \approx 2\pi/\Omega$, we can obtain a useful analytic approximation of numerical solutions for perturbation modes. The condition for the applicability of this weak inhomogeneity approximation (WIA) has the form $\Lambda \ll \Delta$, where Δ is the characteristic scale of spatial inhomogeneity of the system. This condition is almost always satisfied for relaxation oscillations with $\Omega \sim 10^2$ and for higher-order transit modes ($m > 5$).

An analysis of Eqns (3) and (4) shows that under conditions of applicability of WIA, the quantity $\bar{g}(x)$ must be nearly proportional to $W_s(x)$. Hence, it is expedient to introduce a slow variable $\bar{\eta} = \bar{g}/W_s$. The equation for $\bar{\eta}$ has the form

$$\frac{d\bar{\eta}}{dx} = (\bar{\Gamma} + \chi)\bar{\eta} + \bar{w}, \tag{14}$$

where

$$\chi(x) = \frac{q}{G_s} - \frac{1}{W_s}\frac{dW_s}{dx}. \tag{15}$$

Standard solutions of equations of type (3) and (14), expressed in quadratures, do not allow us to establish an explicit relation between the function $\bar{g}(x)$ and $\bar{\eta}(x)$ and $\bar{w}(x)$. For this purpose, it is more convenient to use the operator form of the solution, which can be represented in the form of a series. From Eqn (14), we obtain

$$\bar{\eta}(x) = -\left(1 - \frac{1}{\tilde{\Gamma}}\frac{d}{dx}\right)^{-1}\left(\frac{\bar{w}}{\tilde{\Gamma}}\right) = -\sum_0^\infty\left(\frac{1}{\tilde{\Gamma}}\frac{d}{dx}\right)^n\frac{\bar{w}}{\tilde{\Gamma}}, \tag{16}$$

where $\tilde{\Gamma}(x) = \bar{\Gamma} + \chi(x)$. This series corresponds to the iterative solution of Eqn (14), obtained by using a small parameter $1/\tilde{\Gamma}$. At large oscillation frequencies, the terms of

the series decrease quite rapidly. For a slow variable $\bar{\eta}(x)$, an acceptable accuracy is attained even when we use only the first term in the series:

$$\bar{\eta}(x) = -\frac{\bar{w}}{\bar{\Gamma} + \chi} + V(x), \tag{17}$$

where

$$V(x) = -\frac{\bar{w}}{\bar{\Gamma}^2}\left(\frac{\mathrm{d}}{\mathrm{d}x}\ln\bar{w} - \frac{1}{\bar{\Gamma}}\frac{\mathrm{d}\chi}{\mathrm{d}x}\right) + \ldots \tag{18}$$

are higher-order correction terms. Series (16) and formula (17) describe the 'quasi-homogeneous' particular solution of Eqn (14) that does not contain any oscillations. Denoting in this case the gain perturbation by $\bar{g}_a(x)$, we can present it in the form

$$\bar{g}_a(x) \approx -\frac{W_\mathrm{s}\bar{w}}{\bar{\Gamma} + \chi}. \tag{19}$$

Expression (19) leads to the following type of general solution of Eqn (3) satisfying the boundary condition $\bar{g}(1) = 0$:

$$\bar{g}(x) = \bar{g}_a(x) + \bar{g}_b(x) = -\frac{W_\mathrm{s}(x)\bar{w}(x)}{\bar{\Gamma} + \chi(x)}$$

$$+\frac{W_\mathrm{s}(1)\bar{w}(1)}{\bar{\Gamma} + \chi(1)}\exp\left[-\int_x^1\left(\bar{\Gamma} + \frac{q}{G_\mathrm{s}}\right)\mathrm{d}x\right]. \tag{20}$$

The term $\bar{g}_b(x)$, which is the solution of the homogeneous equation, is proportional to $\exp(\mathrm{i}\Omega x)$ and describes the spatial oscillations of the gain.

An analysis of Eqns (6)–(9) and their numerical solutions shows that in typical situations, the normalised amplitude of the intensity oscillations $w(x)$ remains almost unchanged over the entire aperture of the resonator (Fig. 1). To a good approximation, we can assume it to be independent of x and put, for example, $w = 1$ [in Eqns (3) and (4), the quantities $\bar{g}$ and $\bar{w}$ are defined to within a constant common factor]. The variation of the phase Φ_w of field oscillations is also relatively slow. For quite high-frequency perturbations ($\Omega \gg 1$), the changes in Φ_w over a spatial period Λ are insignificant and the phase Φ_g of gain oscillations manages to 'trace' the slow drift of the phase of field oscillations. Under these conditions, the specific form of the function $\Phi_w(x)$ practically does not affect the magnitude of the phase difference $\Phi = \Phi_g - \Phi_w$ appearing on the right-hand sides of Eqns (6)–(9). A phase shift Φ_w at the resonator aperture leads only to a slight variation in the frequency Ω. In the WIA model, these peculiarities of the amplitude and phase of field perturbations lead to a solution of the boundary value problem for the perturbation modes of the gain $\bar{g}(x)$ in a given field $\bar{w} = w\exp(\mathrm{i}\Phi_w)$ on the basis of relation (20) with boundary condition (5).

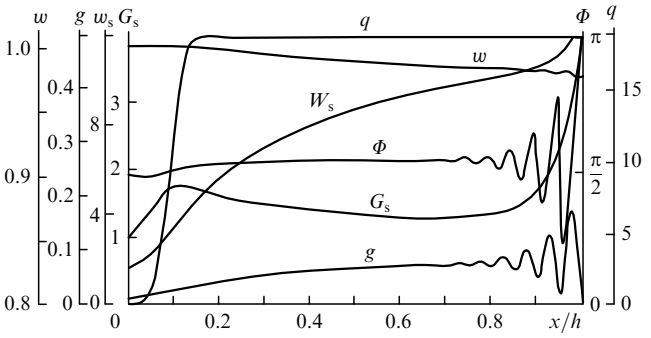

Figure 1. Relaxation mode structure ($\Omega_\mathrm{R} = 125.89$, $\Gamma_\mathrm{R} = 3.23$): steady state profiles of the gain G_s, intensity W_s, and pumping q, and amplitudes of oscillations of the gain g and intensity w; Φ is the phase difference. Calculations were made for $\tau_\mathrm{r} = 0.2$, $q_m = 19$, $\tau_c = 10^{-4}$.

4. Relaxation self-oscillations

Purely relaxation self-oscillations, which are unperturbed by transit resonances, may be excited in a fast-flow laser with quite high pump and relaxation rates. Figure 1 shows a typical spatial structure of the relaxation perturbation mode for this case. The spatial modulation of the gain (edge modulation) emerging at the sharp field gradient at the inlet to the resonator attenuates rapidly and does not reach the optical axis of the resonator. The attenuation condition for gain oscillations [see Eqn (20)], i.e.,

$$\int_0^1\left(\Gamma + \frac{q}{G_\mathrm{s}}\right)\mathrm{d}x \gg 1 \tag{21}$$

is satisfied in this case with a comfortable margin, and hence we can put $\bar{g}(x) = \bar{g}_a(x)$ in the axial region. Taking into account boundary condition (5) at the resonator axis, we arrive at a quadratic equation for complex eigenvalues $\bar{\Gamma}$:

$$\bar{\Gamma} = -\frac{\chi(0)}{2} + \mathrm{i}\left\{\Omega_0^2 - \left[\frac{\chi(0)}{2}\right]^2\right\}^{1/2}. \tag{22}$$

Here, $\Omega_0 = [W_\mathrm{s}(0)/\tau_c]^{1/2}$ is the relaxation frequency [10]. Note that in accordance with Eqns (1) and (2), the quantity $W_\mathrm{s}(0) = q(0) + (\mathrm{d}G_\mathrm{s}/\mathrm{d}x)_{x=0} - \tau_\mathrm{r}^{-1}$ is the rate of formation of inversion and gain at the unstable resonator axis on account of the pump processes, inflow of the excited molecules, and relaxation. In view of the smallness of $\tau_c \sim 10^{-5}$, the relaxation oscillation frequency $\Omega_\mathrm{R} = \mathrm{Im}\,\bar{\Gamma} \approx \Omega_0$. For the increment of relaxation oscillations $\Gamma_\mathrm{R} = \mathrm{Re}\,\bar{\Gamma}$, we obtain

$$\Gamma_\mathrm{R} = -\frac{\chi(0)}{2} = \frac{1}{2}\left[\frac{1}{W_\mathrm{s}(0)}\left(\frac{\mathrm{d}W_\mathrm{s}}{\mathrm{d}x}\right)_{x=0} - q(0)\right]. \tag{23}$$

It follows from Eqn (2) that the relation $[1/W_\mathrm{s}(0)][\mathrm{d}W_\mathrm{s}/\mathrm{d}x]_{x=0} = (\mathrm{d}G_\mathrm{s}/\mathrm{d}x)_{x=0}$ holds at the axis of the unstable resonator. Hence, the condition for the appearance of instability $[1/W_\mathrm{s}(0)][\mathrm{d}W_\mathrm{s}/\mathrm{d}x]_{x=0} > q(0)$ can also be written in the form $(\mathrm{d}G_\mathrm{s}/\mathrm{d}x)_{x=0} > q(0)$. This means that relaxation instability occurs in the case when entrainment of excited molecules by the flow prevails over internal pumping during the formation of inversion at the axis of the unstable resonator. For the conditions corresponding to Fig. 1, when there is no pumping at the axis and the distributions $G_\mathrm{s}(x)$ and $W_\mathrm{s}(x)$ are characterised by considerable gradients in the axial region, numerical computations lead to the value $\Gamma = 3.23$, while the value obtained by calculations using formula (23) is $\Gamma = 3.4$. The value of the frequency Ω_R in both cases is close to $\Omega_0 = 126.23$.

Note that a decline of steady-state distributions $W_s(x)$ and $G_s(x)$ towards the unstable resonator axis is a characteristic feature of almost all lasers with transverse flow of the medium. When there is no pumping at the resonator axis, relaxation-type self-oscillations will be always excited in the resonator in accordance with formula (23). Such a paradoxical conclusion is due to the fact that we have used in our calculations a simplified (single-level) model of the active medium, in which the processes of energy exchange between the levels and components of the working mixture are disregarded. In real lasers, e.g., in a CO_2-N_2 fast-flow laser, these processes lead to pumping of the working transition at the unstable resonator axis.

The instability relaxation mechanism in an unstable resonator with a pump profile of type (13) is associated with a variation in the phase difference Φ of the field and gain oscillations, as a result of which the ratio of phases at the unstable resonator axis becomes favourable for the enhancement of oscillations. Qualitative analysis shows that the movement of the active medium through the region of field with diminishing intensity causes a delay in the phase of gain oscillations as compared to the field oscillations. In its turn, the decrease in the pump rate in the inhomogeneity region also leads to an analogous phase shift. The distribution $\Phi(x)$ is described by an approximate relation following from (19):

$$\Phi(x) = \frac{\pi}{2} + \arctan\frac{\Gamma + \chi(x)}{\Omega}. \tag{24}$$

In the peripheral part of the unstable resonator, where the pumping rate is quite high and the field gradient is insignificant, the quantity $\chi(x)$ is found to be positive as a rule, and the phase difference $\Phi(x) > \pi/2$ for the mode with $\Gamma > 0$. However, it can be seen from (11) that instability arises for a phase difference $\Phi(0) < \pi/2$ at the axis of the unstable resonator. A decrease in the phase difference in the inhomogeneity region below the level $\Phi = \pi/2$ can be seen in Fig. 1. Equation (6) describes the connection between $\Phi(0)$ and the relaxation oscillation amplitude gradient $(dg/dx)_{x=0}$ on the axis of the unstable resonator: $\cos\Phi(0) = (1/2\Omega_0)[(d\ln g/dx)_{x=0} - q(0)]$. Thus, instability arises under the condition $(d\ln g/dx)_{x=0} > q(0)$. For the relaxation oscillations, the quantity $(d\ln g/dx)_{x=0}$ is determined unambiguously by the gradients of the steady state field and gain distributions $(d\ln g/dx)_{x=0} = [1/W_s(0)](dW_s/dx)_{x=0} = (dG_s/dx)_{x=0}$.

The above feedback mechanism for relaxation-type oscillations is essentially of non-resonant type. The oscillation frequency $\Omega_R \approx \Omega_0$ is determined by the steady-state lasing parameters on the unstable resonator axis and can be tuned smoothly by varying these parameters. For active media with a low pump level, when condition (21) is not satisfied, the mode parameters of relaxation oscillations are affected by resonances of transit oscillations. Figure 2 shows the values of Ω and Γ as functions of Ω_0 (the values of Ω_0 were varied by changing the parameter τ_c). The period of the curves is close to 2π, which corresponds to the frequency interval between transit resonances. The maximum values of Γ are attained at frequencies $\Omega = \Omega_R \approx \Omega_0$ [the difference between Ω_R and Ω_0 is manifested in a downward shift of curve (*1*) in Fig. 2a].

It will be shown below that the relaxation frequency in this case coincides with the frequency Ω_m of one of the transit resonances, which is shifted due to pulling. Thus, a 'double resonance' $\Omega = \Omega_R = \Omega_m$ is realised for self-oscillations in this case. The pump rate in Fig. 2a is 2.4 times lower than in Fig. 1, and the effect of transit resonances is still insignificant. For a weak perturbation of the relaxation mode by transit resonances, we can obtain from formula (20) with boundary condition (5) approximate expressions for the frequency and increment:

$$\Omega = \Omega_0 - \frac{\Omega_0}{2}\exp\left[\frac{\chi(0)}{2} - \int_0^1 \chi dx\right]\cos(\Omega_0 - \Delta\Phi_w), \tag{25}$$

$$\Gamma = -\frac{\chi(0)}{2} - \frac{\Omega_0}{2}\exp\left[\frac{\chi(0)}{2} - \int_0^1 \chi dx\right]\sin(\Omega_0 - \Delta\Phi_w), \tag{26}$$

where $\Delta\Phi_w$ is the phase advance of field oscillations at the resonator aperture. The absolute modulation depth of Ω and Γ is found to be the same upon a variation of Ω_0, which is confirmed by numerical calculations (see Figs 2a and b). This fact can be explained graphically by considering the summation of quantities $\bar{g}_a(0)$ and $\bar{g}_b$ in (20) on the complex plane. Upon a further decrease in the pump rate, the effect of transit resonances is enhanced. Frequency jumps (see Fig. 2b) and frequency capture by transit resonances (see Fig. 2c) are observed. In the latter case, the frequencies Ω are found to be localised in quite

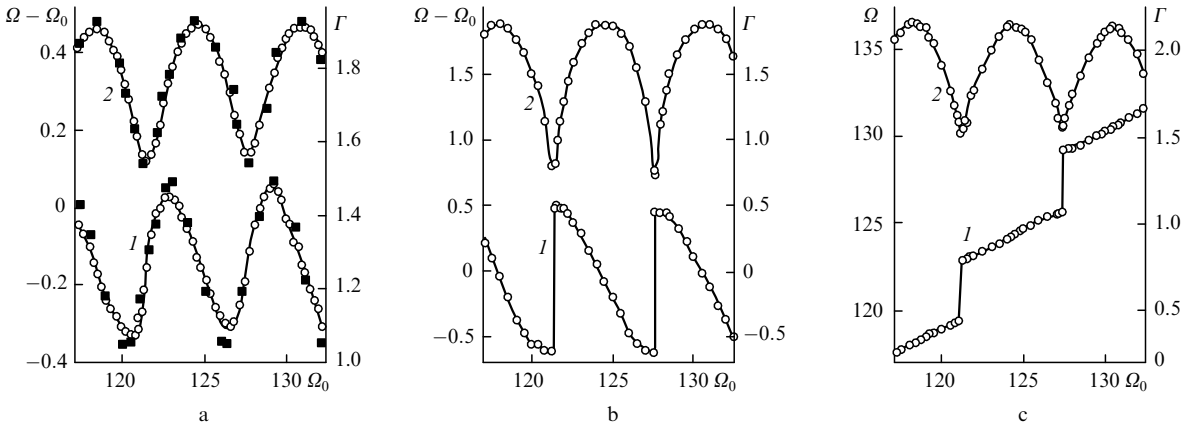

Figure 2. Effect of transit resonances on the frequency Ω [curves (*1*)] and increment Γ [curves (*2*)] of the relaxation mode for (a) $\tau_r = 0.5$, $q_m = 8$ (dark squares correspond to calculations by (25), (26)); (b) $\tau_r = 0.65$, $q_m = 6.15$ and (c) $\tau_r = 1$, $q_m = 4$.

narrow intervals in the vicinity of Ω_m. Under the conditions of strong interaction of self-oscillations, their division into relaxation and transit parts becomes meaningless. In such a case, it is more appropriate to speak of mixed type of oscillations.

5. Transit edge self-oscillations

Resonance properties of the feedback sustaining transit oscillations are caused by the spatial modulation of the gain due to field discontinuity at the mirror edge at the inlet to the resonator. Hence these self-oscillations may be called transit edge oscillations. Such a feedback is effective only in a medium with a quite slow relaxation ($\tau_r \leqslant \tau_f$) and a moderate pump level ($q_m < 1$). In this case, the edge modulation propagates towards the unstable resonator axis so that the boundary condition for $\bar{g}$ is satisfied at the axis. The transit oscillation modes can be calculated in most cases with boundary conditions (12). The characteristic features of the spatial structure of transit modes are their quasi-periodicity, sawtooth distribution of the phase difference Φ, and the presence of nodal points at which $g \approx 0$ (Fig. 3). At these points, the initial unperturbed state of the medium at the input to the resonator is reproduced approximately.

Figure 4 shows the space–time structure of perturbation of the gain $\tilde{g}(x,t)\mathrm{Re}[\bar{g}(x)\exp(\bar{\Gamma}t)]$ of the transit edge mode with $m = 5$. The perturbation of $\tilde{g}(x,t)$ can be presented as a superposition of an attenuating travelling wave propagating towards the unstable resonator axis and the quasi-homogeneous 'component' oscillating in time. In expression (20), this component corresponds to the terms $\bar{g}_b(x)$ and $\bar{g}_a(x)$. Such a peculiar type of wave movement is characterised by

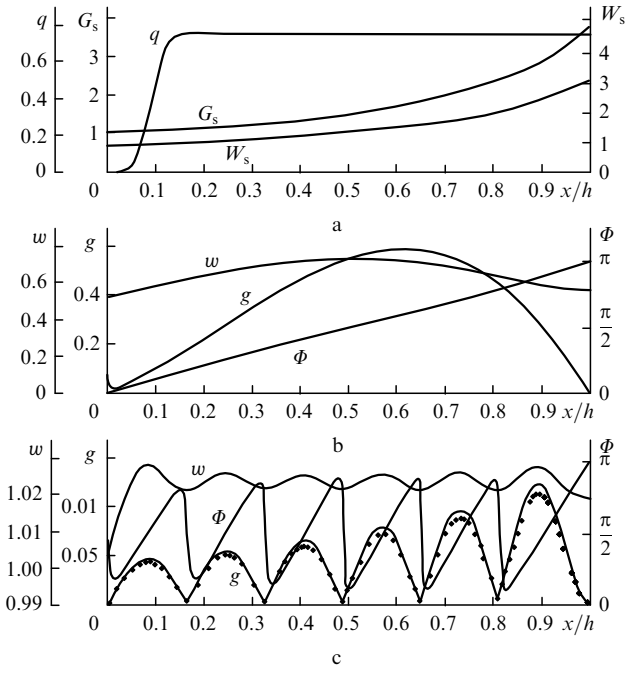

Figure 3. (a) Structure of edge transit modes: steady state profiles of the gain G_s, intensity W_s, and pumping q, as well as structures of (b) first ($\Omega_m = 7.45$, $\Gamma_m = 0.63$) and (c) sixth ($\Omega_m = 37.68$, $\Gamma_m = 0.86$) transit modes: amplitudes of the gain g and intensity w; Φ is the phase difference. Calculations were made for $\tau_r = 5$, $q_m = 0.8$, $\tau_c = 10^{-4}$. Dark points correspond to analytic calculations.

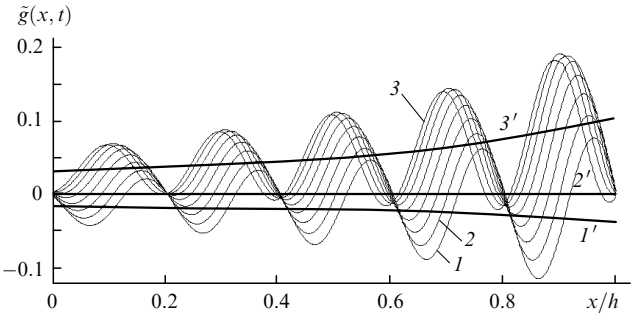

Figure 4. Gain perturbation wave (fifth edge transit mode, $\Omega_m = 31.86$, $\Gamma_m = 0.82$). The gain profiles $\tilde{g}(x,t)$ are shown at different instants of time with an interval of $0.01\tau_f$ [curve (*1*) corresponds to the initial instant]. Curves (*1′*, *2′*, *3′*) are quasi-homogeneous 'components' corresponding to curves (*1*, *2*, *3*).

the presence of stationary nodes separated, in contrast to an ordinary standing wave, by the spatial period $\Lambda_m \approx 2\pi/\Omega_m$ of the travelling wave.

Expression (20) with the quasi-stationary boundary condition $\bar{g}(0) = 0$ can be used to derive a relation for the complex increment $\bar{\Gamma}$:

$$\frac{\bar{\Gamma} + \chi(1)}{\bar{\Gamma} + \chi(0)} = \frac{W_s(1)}{W_s(0)} \exp\left[-\bar{\Gamma} + i\Delta\Phi_w - \int_0^1 \frac{q}{G_s} dx \right]. \qquad (27)$$

For transit modes of sufficiently high orders, we can assume that $\Omega_m \gg |\chi|$ and obtain from Eqn (27)

$$\Omega_m = 2\pi m + \Delta\Phi_w + \frac{\Delta\chi}{2\pi m}, \qquad (28)$$

$$\Gamma_f = \ln\frac{W_s(1)}{W_s(0)} - \int_0^1 \frac{q}{G_s} dx, \qquad (29)$$

where $\Delta\chi = \chi(1) - \chi(0)$. The last term in (28) can be omitted. Due to the phase shift $\Delta\Phi_w \sim 1$, the frequency Ω_m is not exactly a multiple of 2π. Expression (29) was derived in [4] for a particular type of an unstable resonator. This expression reflects the fact that in accordance with (19) and (20), the ratio $g_b(1)/g_b(0)$ of amplitudes of spatial oscillations of the gain at the resonator inlet and on its axis must be equal to the ratio of amplitudes of intensity oscillations, which is approximately equal to $W_s(1)/W_s(0)$. The decrease in the field towards the unstable resonator axis is a necessary condition for instability. Pumping causes attenuation of spatial modulation and hence prevents instability. A comparison with numerical computations shows that expression (29) describes quite correctly the increments of transit modes with $m > 5$ away from the relaxation resonance ($\Omega_m \ll \Omega_0$). Thus, for the mode with $m = 6$ (see Fig. 3b), the value obtained by calculations using expresion (29) is $\Gamma_m = 0.82$, while numerical calculations lead to the value $\Gamma_m = 0.86$. The spatial mode structure is also approximated quite well by relation (20). For lower-order modes, the accuracy of analytic calculations becomes lower.

Expression (29) pertains to an unstable resonator with a sharp edge of the mirrors. Under actual conditions, the field gradient at the inlet to the resonator is smoothed [11], which leads to an attenuation of the edge modulation and hence to a lowering of the transit mode increments. This can be seen

from a comparison of Figs 5a and b. [Smoothing was simulated by introducing additional losses into the narrow ($\delta = 0.05$) region at the edge of the unstable resonator aperture.] Higher-order modes, for which the quasi-period Λ_m becomes comparable with the quantity δ, are suppressed more strongly. These data emphasise the important role of the edge modulation in the mechanism of transit self-oscillation excitation. Note that a complete suppression of edge modulation is possible in the case when a perturbed flow is incident at the unstable resonator inlet at gain oscillations are matched with field oscillations in such a way that the boundary condition $\bar{g}_{\text{in}} = \bar{g}_a(1)$ is satisfied at the inlet. This is possible in a system consisting of an unstable resonator and a multipass amplifying cell placed upstream. In actual fast-flow lasers, the quasi-periodic spatial structure of transit modes can also be smoothed due to turbulent mixing of the gas in the active medium flow. The resulting decrease in the mode increment depends on the relation between the spatial period Λ_m and the characteristic size of turbulent vortices in the flow. The decrease in increments is most pronounced for higher-order modes, which is in accord with the results obtained in [5], where the effect of velocity spread in the flow on the self-oscillation increments was calculated.

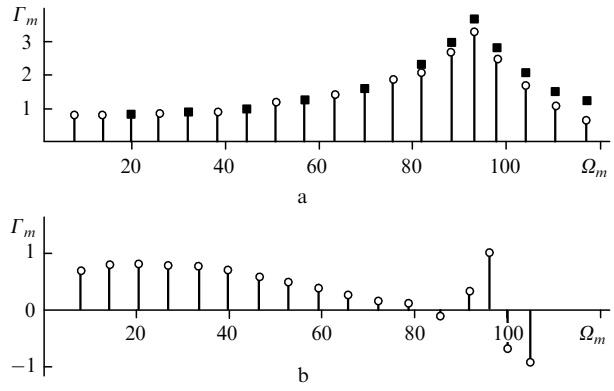

Figure 5. Frequencies Ω_m and increments Γ_m of edge transit modes for $\tau_r = 5$, $q_m = 0.8$, $\tau_c = 10^{-4}$ in the case of an unstable resonator with (a) a sharp mirror edge and (b) a mirror with a smoothed edge. Dark squares correspond to calculations made by (30).

Figure 5a illustrates the effect of the relaxation resonance on the transit mode characteristics. The figure shows the mode frequencies and increments for the case when Ω_0 coincides with the frequency of the mode with $m = 15$. For modes with $m > 5$, an increase in the increments is observed as the mode frequency approaches Ω_0. The maximum value Γ_m is attained when the frequencies Ω_m and Ω_0 coincide. In the region $\Omega_m > \Omega_0$, the mode increments decrease rapidly. The narrowing of the frequency intervals between the modes adjoining Ω_0, which is a result of transit mode frequency pulling by the relaxation resonance, is worth noting. The analytic model gives an approximate relation connecting the frequencies and increments of the interacting modes:

$$\exp[-2(\Gamma_m - \Gamma_f)] = \left[\frac{2(\Gamma_m - \Gamma_R)}{\Omega_0}\right]^2 + \left(1 - \frac{\Omega_m^2}{\Omega_0^2}\right)^2, \quad (30)$$

where Γ_R and Γ_f are the increments of unperturbed relaxation and transit modes defined by expressions (23) and (29). The dependence $\Gamma_m(\Omega_m)$ obtained from relation (30) is in good agreement with numerical calculations (Fig. 5a). In the frequency resonance region ($\Omega_m = \Omega_0$), the increments become considerably larger. It follows from Eqn (30) that positive increments Γ_m in resonance are also possible in the case when both values (Γ_R и Γ_f) are negative.

Figure 6 illustrates the variation of frequency and increment of a fixed transit mode with $m = 11$ during tuning of Ω_0. These data, as well as the data presented in Fig. 5, show that the range of interaction between the relaxation and transit modes is quite wide and embraces ~ 10 frequency intervals between transit modes. One can see from Fig. 6 that the transit mode frequency is pulled downwards by the relaxation resonance. The maximum value of the frequency shift is close to π, i.e., half the mode interval. For frequency resonance ($\Omega_m = \Omega_0$), the frequency shift Ω_m is half the maximum value, i.e., is of the order of $\sim \pi/2$. The increment of mode Γ_m attains its maximum value in this case. In the limit $\Omega_0 \to \infty$, the value of Γ_m approaches the value $\Gamma_f = 0.86$ calculated for an unperturbed transit mode. The same value is attained for $\Omega_0 \approx \Omega_m/\sqrt{2} \approx 48$. A kink in the curve $\Gamma_m(\Omega_0)$ is observed at this point; upon a further decrease in Ω_0, the increments decrease rapidly and soon become negative. These peculiarities in the behaviour of the curves in Fig. 6 are associated with changes in the spatial structure of the mode caused by tuning of the relaxation resonance frequency. These variations can be explained quantitatively by the analytic model which is not presented here.

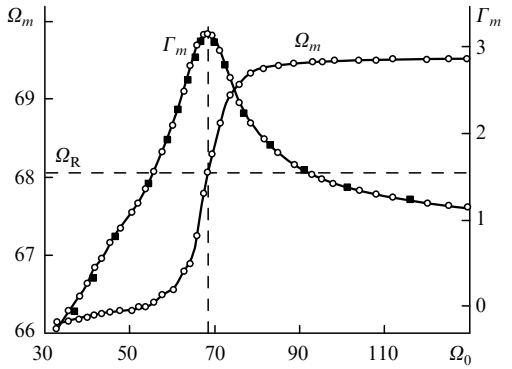

Figure 6. Effect of the relaxation resonance on frequency Ω_m and increment Γ_m of the 11th transit edge mode for $\tau_r = 5$, $q_m = 0.8$. Dark squares correspond to calcualtions made by (30).

6. Intrinsic transit self-oscillations

The feedback mechanisms in lasers with high pump and relaxation rates becomes ineffective due to edge modulation. However, spatial modulation of the gain can also appear in the region adjoining the unstable resonator axis for high internal gradients of the parameters of the system. Because the transit time through this region is $\tau'_f \ll \tau_f$, these oscillations may reach the unstable resonator axis and ensure a positive feedback. As in the case of edge transit oscillations, this feedback is also resonant. The frequency of the lowest intrinsic transit mode is $\Omega \approx 2\pi/\tau'_f$. Because the intrinsic field gradients are not as high as the edge gradient, modulation of the gain is much weaker than the edge modulation. Figure 7 shows the structure of the lowest

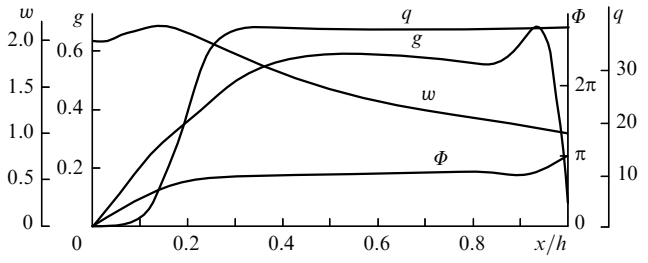

Figure 7. Structure of the first intrinsic transit mode ($\Omega = 27.5$, $\Gamma = 4.47$): amplitudes of the gain g and intensity w, as well as the phase difference Φ and pump profile q for $\tau_r = 0.2$, $q_m = 37$, $\tau_c = 0$.

intrinsic transit mode with frequency $\Omega = 27.5$. The pump rate is increased and corresponds approximately to an eightfold increase over the threshold value. In spite of a small depth of the spatial modulation, the increment of this mode is quite high ($\Gamma = 4.47$).

The frequency ranges of the intrinsic and edge transit modes overlap, and these types of oscillations can interact with each other. Figure 8 shows the frequencies and increments of mixed self-oscillations appearing due to such an interaction. The pump rate in this figure is much lower than in Fig. 7, and hence the edge modulation of the gain reaches the resonator axis. However, it can be seen from the figure that the increments of unperturbed intrinsic modes remain negative. In the range of intrinsic transit resonances with $m = 1$ and 2, the increments increase and instability sets in. Note that for a high degree of pumping nonuniformity, the WIA model becomes inapplicable. This is manifested in Fig. 7 in that the perturbation amplitude of the field $w(x)$ changes quite strongly at the resonator aperture. At the same time, the WIA model may be applicable for calculating mixed self-oscillations in unstable resonators with a moderate pump rate when the next terms of series (16) are included in relation (19).

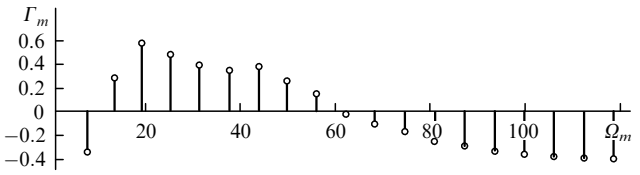

Figure 8. Frequencies and increments appearing upon the interaction of intrinsic and edge transit modes for $\tau_r = 0.5$, $q_m = 4$, $\tau_c = 0$.

7. Conclusions

We have shown that self-oscillation instability in fast-flow unstable resonator lasers is quite complicated due to different mechanisms and various types of instabilities that can interact with one another. In all cases, the instability mechanisms are associated with the presence of spatial gradients of steady-state lasing parameters (pump rate, field strength, and gain) in the resonator or at the input to the resonator. The transit self-oscillations are excited by the field jump at the edge of the unstable resonator aperture, which leads to spatial modulation of the gain perturbation. The latter is an indispensable feature of transit modes since it ensures the fulfilment of the boundary condition on the unstable resonator axis. The application of mirrors with a smoothed edge suppresses the edge modulation and lowers the increments of transit modes. Relaxation instability is associated with the presence of gradients in the vicinity of the unstable resonator axis. Calculations show that self-oscillation increments at frequencies close to the relaxation frequencies Ω_0 in lasers with a moderate internal pump rate may substantially increase due to interaction between transit and relaxation mechanisms. Interaction of intrinsic transit self-oscillations with edge transit and relaxation self-oscillations also leads to a considerable increase in the increments. The results of our studies may be useful for developing methods of suppressing self-oscillation instability in fast-flow lasers, as well as methods of controlling temporal lasing parameters [6].

Acknowledgements. This work was supported by the Russian Foundation for Basic Research (Grant No. OFI-A 05-02-08-244).

References

1. Dreizin Yu.A., Dykhne A.M. *Pis'ma Zh. Eksp. Teor. Fiz.*, **19**, 718 (1974).
2. Dreizin Yu.A., Dykhne A.M., Napartovich A.P., Panchenko Yu.M., in *Abstracts of Papers of II All-Union Symposium on the Physics of Gas Lasers* (Moscow: Nauka, 1975) p. 26.
3. Alme M.L. *Appl. Phys. Lett.*, **29**, 35 (1976).
4. Likhanskii V.V., Napartovich A.P. *Kvantovaya Elektron.*, **7**, 237 (1980) [*Sov. J. Quantum Electron.*, **10**, 139 (1980)].
5. Likhanskii V.V., Napartovich A.P. *Izv. Akad. Nauk SSSR. Ser. Fizich.*, **45**, 399 (1981).
6. Mushenkov A.V., Odintsov A.I., Sarkarov N.E., Fedoseev A.I., Fedyanovich A.V. *Kvantovaya Elektron.*, **24**, 431 (1997) [*Quantum Electron.*, **27**, 419 (1997)].
7. Artamonov A.V., Naumov V.G. *Kvantovaya Elektron.*, **4**, 178 (1977) [*Sov. J. Quantum Electron.*, **7**, 101 (1977)].
8. Dmitriev K.I., Kallubinskaya T.A., Kutsenko A.I., Pavlov S.P., Panasyuk V.F., Sokolov N.A. *Kvantovaya Elektron.*, **18**, 1372 (1991) [*Sov. J. Quantum Electron.*, **21**, 1258 (1991)].
9. Mushenkov A.V., Odintsov A.I., Fedoseev A.I., Fedjanovich A.V. *Proc. SPIE Int. Soc. Opt. Eng.*, **4644**, 307 (2002).
10. Khanin Ya.I. *Dinamika kvantovykh generatorov* (Laser Dynamics) (Moscow: Sov. Radio, 1975).
11. Anan'ev Yu.A. *Opticheskie rezonatory i problema raskhodimosti lazernogo izlucheniya* (Optical Resonators and the Problem of Divergence of Laser Radiation) (Moscow: Nauka, 1979).